



Infrasound Analysis of Saare Wind Energy Windfarm

100 Vestas V236–15 MW turbines
Physics-based full-wave modeling using SoundSim360

Prof. Ken Mattsson
Professor of Scientific Computing
Uppsala University

Chief Executive Officer
Pronumerix AB

May 17, 2026

Executive Summary

On behalf of the resident initiative (SRS), we have conducted a comprehensive analysis of infrasound dispersion in the area surrounding the proposed Saaremaa Offshore Wind Farm described in the Environmental Impact Assessment (EIA) documents submitted by *Saare Wind Energy OÜ* [37, 38]. The assessed project consists of 100 Vestas V236–15 MW turbines with a hub height of 145 m.

In addition to the infrasound analysis, we have also performed a corresponding dBA-based noise study to facilitate comparison with the environmental assessments presented in the EIA documentation [38]. The EIA documents discuss a nighttime guideline value of approximately 35 dBA for sensitive residential and recreational environments. However, since this metric is based on A-weighted sound pressure levels, low-frequency and infrasonic components are strongly attenuated in the assessment. This motivates complementary analyses using full-wave physics-based modeling with *SoundSim360*.

The sound propagation models currently used in environmental permitting, most notably *Nord2000* and *ISO 9613-2*, were not originally developed for large-scale offshore wind turbine noise assessment and exhibit important limitations when applied to modern turbines. In particular, these models have limited capability to represent infrasonic and low-frequency, amplitude-modulated sound propagation under realistic atmospheric conditions. As a consequence, sound levels may be underestimated during meteorological situations known to enhance long-range propagation, such as nighttime temperature inversions and strong wind shear.

Furthermore, the widespread reliance on A-weighted sound pressure levels (dBA) introduces methodological limitations when assessing low-frequency sound and infrasound. The A-weighting filter strongly attenuates low-frequency and infrasonic components, despite increasing scientific evidence suggesting that such frequencies may contribute to human perception, annoyance, sleep disturbance, and physiological responses in sensitive individuals.

Reliable exposure assessment therefore requires both measurements and simulations that encompass the full relevant frequency range, extending at least down to 0.1 Hz. In this study, we employ *SoundSim360*, a physics-based numerical framework that resolves the three-dimensional acoustic wave field without reliance on empirical correction factors or user-adjustable tuning parameters. This enables internally consistent comparisons between measured and simulated sound fields and provides a more physically transparent basis for environmental impact assessment than current regulatory practice.

Disclaimer: This report has been prepared by Pronumerix AB and represents an independent expert assessment by the author. The analyses are based on peer-reviewed research, scientific literature, numerical simulations, and measurement methodologies developed in collaboration with researchers at Uppsala University and published in the scientific literature. References to Uppsala University describe the academic background of the research but do not imply institutional endorsement of the conclusions or recommendations presented in this report.

High-fidelity modeling of wind turbine noise using *SoundSim360*

Drawing on detailed measurements from several wind farms, including Målarberget and Lervik, we have calibrated a high-precision computational tool, **SoundSim360** [26], capable of simulating sound propagation over

complex terrain and across the full frequency spectrum, including infrasound (frequencies below 20 Hz).

Sound propagation over large distances is governed by a range of interacting physical processes, including atmospheric stratification, topography, ground impedance, source geometry, and spectral content. Accurate modeling must therefore capture key physical phenomena such as diffraction, refraction, geometric scattering, absorption, transmission, reflection, and interference. If these processes are not represented correctly, noise dispersion cannot be reliably simulated. *SoundSim360* addresses these challenges by solving the full three-dimensional acoustic wave equation, incorporating real atmospheric profiles and high-resolution terrain data, with no user-adjustable “free parameters.” This ensures that simulation accuracy depends solely on the correctness of the physical input data, not on subjective calibration.

Over the past two decades, our research group has developed a suite of advanced numerical methods specifically for high-fidelity sound propagation modeling (see, e.g., [21, 30, 22, 27, 28, 20, 23, 3, 19, 24, 36, 25, 31, 18, 2, 45, 44, 29, 34]). These methods form the foundation of *SoundSim360*, which is implemented for efficient execution on modern high-performance graphics processors (GPUs), enabling detailed full-wave simulations of large acoustic domains. For details about *SoundSim360* we refer to [26].

In contrast, the most widely used model for wind turbine noise prediction today is *Nord2000* [1], commonly implemented in commercial software such as *SoundPlan* and *windPRO*. *Nord2000* is fundamentally a ray-tracing model based on the assumption of high-frequency sound propagation. As a two-dimensional approximation, it cannot accurately represent low-frequency propagation, nor can it model interference between multiple sources. Its treatment of diffraction is also limited, which is particularly problematic in hilly terrain or near buildings and barriers. Previous work has demonstrated that *Nord2000* yields unreliable results in complex terrain [3]. To mitigate these shortcomings, the model introduces numerous empirical “tuning” parameters, making results heavily dependent on user settings and assumptions. Several independent studies, including those by Conny Larsson [15], show that *Nord2000* systematically underestimates measured sound levels by 5–7 dBA at approximately 1 km distance. Even more simplified models, such as the *ISO 9613-2* standard [10], generally produce similar or less accurate results.

All of these traditional (simplified) models face inherent difficulties when simulating low-frequency or infrasonic sound, particularly over long distances and in non-flat terrain. Their reliance on user-adjustable correction factors introduces substantial uncertainty, which increases with turbine number, terrain complexity, and propagation distance. Because low-frequency and infrasonic components are only weakly attenuated by air and ground, they can travel many kilometers, making these modeling limitations especially critical.

For a computational tool to be broadly useful to the scientific and engineering community, it must satisfy three core criteria: 1) the underlying methodology must be rigorously validated and transparently documented; 2) results must be clear, interpretable, and visually accessible; and 3) the tool must be robust and user-independent, avoiding ad hoc parameter tuning.

These principles define the design philosophy of *SoundSim360*. Unlike conventional ray-tracing models such as *Nord2000*, which depend on empirical adjustments, *SoundSim360* directly solves the full three-dimensional acoustic wave equation, thereby eliminating the main sources of uncertainty. The four key deficiencies of ray-tracing approaches that our method overcomes are: 1) inadequate treatment of low-frequency sound (below 200 Hz), 2) difficulty in resolving complex geometries, 3) limited capacity to simulate sound transmission through structures, and 4) inability to capture transient or amplitude-modulated sources.

As an illustrative example, Figure 1 presents a comparison between *SoundSim360* and *Nord2000* (as implemented in *SoundPlan 9.1*) for a 31.5 Hz monopole source located at Polacksbacken, Uppsala University. The source is positioned 10 m above ground with a sound power level of 105 dB. Terrain and building data were obtained from Lantmäteriet [14], and the ground was modeled as a hard surface (impedance class H in *Nord2000*). All other *Nord2000* parameters were kept at default values. The resulting sound pressure level (SPL) distribution at 2 m height is shown for both models. The computational domain for *SoundSim360* spans 500 m × 600 m × 250 m. Significant discrepancies are evident in the shadow regions behind buildings, where *Nord2000* systematically underestimates SPL by approximately 20–30 dB. These deviations reflect the fundamental limitations of ray-tracing methods in the low-frequency regime and highlight the necessity of full-wave simulation approaches for accurate modeling of wind turbine noise.

Measured Infrasound and Low-Frequency Noise from Wind Turbines

Long-term exposure to environmental noise has been associated with an increased risk of cardiovascular disease [6, 50], which remains the leading cause of mortality in Western Europe. Low-frequency noise is of particular concern due to its long-range propagation characteristics and limited attenuation by typical building structures.

In practice, regulatory assessment often relies on facade-level calculations performed in software such as *windPRO*, followed by subtraction of tabulated facade attenuation values [12]. The general applicability of such attenuation models has been questioned in the acoustic literature [33], and the limited public availability of detailed turbine source spectra restricts independent verification of low-frequency calculations.

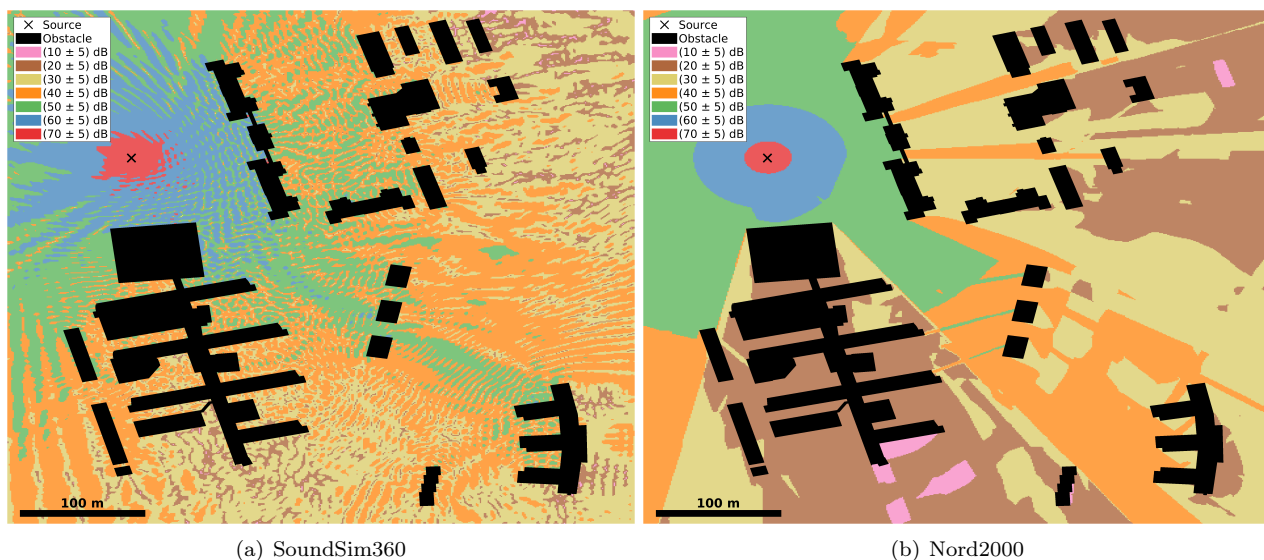


Figure 1: Low-frequency (31.5 Hz) sound simulation at Polacksbacken (105 dB point source at \times , 10 m above ground), comparing (a) SoundSim360 and (b) Nord2000. Shown are sound pressure levels 2 m above ground. Nord2000 cannot accurately model edge diffraction at low frequencies.

For physically meaningful assessment, wind turbine noise should be evaluated using broadband spectral analysis across third-octave bands (f_c) spanning the full audible and infrasonic range (approximately 0.1 Hz to 20 kHz). However, environmental assessments typically report octave-band data only within 31–10,000 Hz, thereby excluding infrasonic and very low-frequency components that are increasingly relevant for modern large-scale turbines.

Previous studies by Møller and Søndergaard [32, 43] demonstrated that the relative contribution of low-frequency noise increases with turbine size. This reflects a downward spectral shift in acoustic emission, implying that larger turbines emit a greater proportion of their energy in the low-frequency and infrasonic range. Recent large-scale measurement campaigns confirm this trend [49].

Wind turbine noise spectra are frequently dominated by low-frequency components, with substantial energy below 10 Hz. Peak spectral energy has often been observed below 1 Hz, and scaling relations indicate that these components increase with rotor diameter and blade length. Under such conditions, evaluation based solely on *A-weighted* sound pressure levels (dBA) becomes physically limited, as the A-weighting curve strongly attenuates frequencies below approximately 20 Hz. Alternative weighting filters, such as *C*- and *G*-weighting, provide improved sensitivity to low-frequency and infrasonic sound, but still do not fully represent total acoustic energy in this range (see Figure 2).

Field measurements of infrasound were conducted at the Målarberget wind farm on 23 October 2024 during both turbine operation and turbine shutdown caused by negative electricity market prices (Figure 2). The results show that turbine operation was the dominant local source of infrasound. The broadband level within 1–20 Hz was approximately 27 dB lower during turbine shutdown compared to operational conditions. Comparable results were obtained at the Lervik wind farm on 21 May 2024.

Summation of third-octave bands within 1–20 Hz yields a broadband infrasound level of approximately 106.4 dB during turbine operation. This corresponds to weighted levels of approximately 22.7 dBA, 73.9 dBC, and 92.1 dBG. During turbine shutdown, the corresponding levels were 79.1 dB (unweighted), -2.8 dBA, 44.5 dBC, and 59.3 dBG. These results highlight the strong dependence of assessed noise levels on the choice of frequency weighting.

Frequencies below approximately 1 Hz were not included in the measurements due to current instrumentation limitations. However, both numerical modeling and field observations indicate that peak spectral energy may occur in the range 0.2–0.6 Hz, depending on turbine design and operating conditions.

Several independent studies report that indoor infrasonic levels are often 3–5 dB higher than corresponding outdoor levels [13, 4, 5, 7]. This is typically attributed to structural coupling and resonance effects within buildings, which can amplify low-frequency pressure fluctuations. These findings emphasize the importance of explicitly considering indoor exposure when evaluating potential human response to wind turbine infrasound.

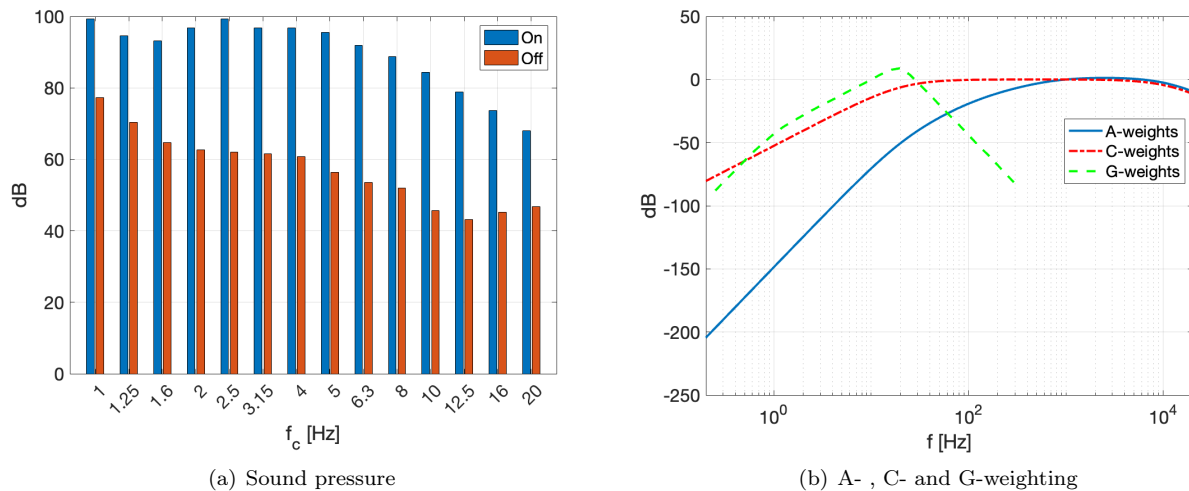


Figure 2: (a) Measured infrasound levels during wind turbine operation and during turbine shutdown, demonstrating the turbine contribution to low-frequency sound. (b) Frequency-dependent attenuation introduced by A-, C-, and G-weighting filters, illustrating their effect on low-frequency and infrasonic sound levels.

Instrumentation and Calibration for Infrasound Measurements

Accurate measurement of infrasound at frequencies approaching, and extending below, 1 Hz requires instrumentation that is demonstrably calibrated within this frequency range. Reliable calibration near 1 Hz can be performed at **NORSAR** using their Hyperion reference system at the certified CTBTO infrasound monitoring station in Elverum, Norway.

In this study, we employed four **Lidström infrasound microphones**, originally developed in Sweden during the early 1980s for helicopter detection applications [17]. These sensors are characterized by high sensitivity and mechanical robustness, making them well suited for long-term outdoor measurements. They have previously been used by the Swedish Defence Research Agency (FOI), the Royal Institute of Technology (KTH), and are currently operated by the Swedish Institute of Space Physics (IRF) in Kiruna under the supervision of Johan Kero [48]. Three of the microphones were provided through collaboration with IRF. All four sensors were calibrated at NORSAR against the Hyperion reference system prior to deployment.

During the field campaigns, we also evaluated commercial sound level meters, including the **Nor140** and **Nor145**, which are commonly used in environmental noise assessments. Although manufacturer specifications indicate sensitivity down to approximately 0.4 Hz for the Nor145 instrument, our comparative measurements indicate reduced accuracy at very low frequencies. Below approximately 3 Hz, measured levels deviated significantly from those obtained using reference-calibrated sensors. This highlights the importance of verified low-frequency calibration when conducting infrasound measurements. Instruments not calibrated near 1 Hz may therefore introduce substantial uncertainty in wind turbine infrasound assessments.

Reliable infrasound monitoring consequently requires professionally calibrated sensors. Commercial systems from manufacturers such as **Hyperion** and **Chaparral** enable accurate measurements over the approximate frequency range 0.1–200 Hz. To further improve measurement accuracy below 1 Hz, two Hyperion microphones have recently been incorporated into our measurement system. Indoor measurements are also important, as building structures can modify and, in some cases, amplify low-frequency pressure fluctuations through structural coupling and resonance effects.

The measurement campaigns used to calibrate and validate our numerical propagation model, and to estimate infrasound source strength through inverse modeling, were conducted at two wind farms: the **Lervik wind farm** (21 May 2024 and 10 September 2024) and the **Målarberget wind farm** (26 October 2023, 23 October 2024, and 16 December 2024). At each site, measurements were performed at one to three receiver locations. Concurrent atmospheric data were recorded during each campaign and incorporated into the inverse modeling procedure. Access to operational turbine data, including turbine on/off status, was essential for accurate interpretation and was provided through cooperation with the respective wind farm operators.

A detailed description of the measurement methodology, calibration procedures, and dataset is presented in [26]. Measurement data are available upon reasonable request. The turbines at *Målarberget* are **Vestas V150–4.3 MW** units, while those at *Lervik* are **SG170–6.6 MW** turbines. Averaging results across five independent campaigns yields an estimated sound power level of approximately 163 dB at 1 Hz. These findings underscore the importance of using properly calibrated instrumentation when assessing infrasound from wind turbines, as inadequate calibration may lead to systematic underestimation of exposure levels.

Audible Sound Propagation (dBA) at Saare Wind Energy Windfarm

The project comprises 100 proposed Vestas V236–15 MW turbines with a hub height of 145 m. A sound power level of approximately 115.3 dBA per turbine was assumed, consistent with the A-weighted noise emission map presented in [38]. An uncertainty of approximately ± 3 dB should be assumed due to atmospheric variability, operational conditions, and source characterization, consistent with the uncertainty discussion presented in [38].

Simulations were performed using a representative nighttime atmospheric profile (31 March 2023, 04:00 AM; meteorological data obtained from the THREDDS Data Server), corresponding to stable atmospheric conditions with a tailwind of 8 m/s referenced at 10 m above ground level. Such conditions are known to enhance long-range sound propagation. Ground properties were modeled according to the Nord2000 classification scheme [1], with soft surfaces represented by impedance class E and hard surfaces (e.g., water, asphalt, and concrete) treated as fully reflecting (class H). Atmospheric attenuation was implemented according to ISO 9613-1 [9].

The resulting spatial distribution of A-weighted sound pressure levels is shown in Figure 3, while corresponding levels at representative receptor locations are summarized in Table 1.

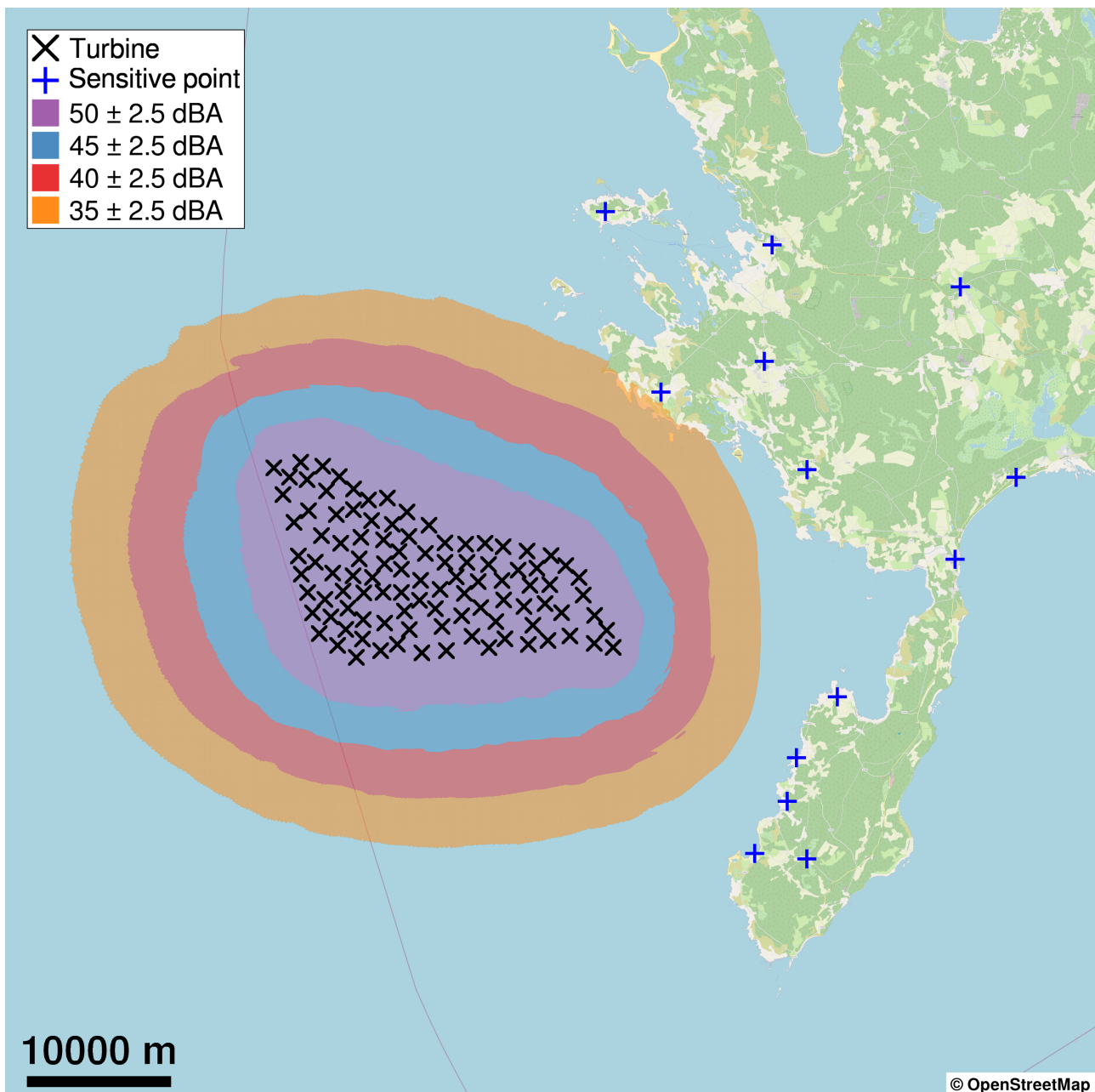


Figure 3: Simulated A-weighted sound pressure levels (dBA) calculated using *SoundSim360* under tailwind conditions of 8 m/s and a representative nighttime atmospheric profile.

Location	x-coordinate	y-coordinate	SPL [dBA]	Nearest turbine [m]
Vilsandi	373505	6473120	20.1	24127
Kihelkonna	384964	6470470	14.8	26427
Kärla	397891	6467211	5.0	33247
Lümanda	384178	6462440	22.9	19753
Karala	376960	6460525	31.2	13682
Kotlandi	386928	6454850	24.5	17523
Mändjala	401418	6453922	7.6	30382
Salme	397038	6448346	13.8	24567
Rahuste	388585	6438994	24.3	15993
Kaunisppe	385619	6434842	25.8	14911
Jämaja	384881	6431822	24.7	16194
Türju	382501	6428239	24.2	17436
Iide	386132	6427762	19.4	19996

Table 1: A-weighted sound pressure levels (dBA) at the sensitive receptor points, calculated using *SoundSim360*. Results are shown for downwind conditions with a wind speed of 8 m/s under a representative nighttime atmospheric profile. A turbine sound power level of $115.3 + 3$ dBA was assumed.

Our simulations indicate slightly higher A-weighted sound pressure levels along portions of the shoreline compared to those presented in the EIA documentation, although the predicted levels remain below the 35 dBA nighttime guideline discussed in [38].

The calculations are based on manufacturer-provided sound power data from Vestas. However, several independent field studies have reported systematic discrepancies between predicted and measured A-weighted sound pressure levels, particularly under stable nighttime atmospheric conditions where long-range propagation may be enhanced.

Of particular interest is amplitude-modulated (AM) noise [15], which frequently occurs during evening and nighttime conditions. AM introduces a characteristic time-varying “swishing” or pulsating sound that may propagate over distances exceeding 10 km under favorable atmospheric conditions. When pronounced AM occurs, short-term peak levels may exceed stationary model predictions by several dBA. Since this phenomenon is generally not explicitly represented in standard steady-state emission maps, it may contribute to underestimation of perceptual annoyance and nighttime disturbance in conventional regulatory assessments.

Infrasound Propagation at Saare Wind Energy Windfarm

The project comprises 100 proposed Vestas V236–15 MW turbines with a hub height of 145 m. A sound power level of 163 dB at 1 Hz was assumed for each turbine. This source strength is consistent with values inferred from independent field measurements of modern large-scale turbines (**Vestas V150–4.3 MW** and **SG170–6.6 MW**) reported in [26]. The levels are most likely higher due to the increased effect.

Simulations were performed using a representative nighttime atmospheric profile (31 March 2023, 04:00 AM; meteorological data from the THREDDS Data Server), corresponding to stable atmospheric conditions with a tailwind of 8 m/s (referenced at 10 m above ground level). Such conditions are known to enhance long-range sound propagation. Ground properties were modeled following the Nord2000 classification scheme [1], with soft surfaces represented as impedance class E and hard surfaces (e.g., water, asphalt, concrete) as fully reflecting (class H). Atmospheric attenuation was implemented according to ISO 9613-1 [9].

The resulting spatial distribution of the 1 Hz infrasound field is shown in Figure 4, with corresponding sound pressure levels at representative receptor locations summarized in Table 2.

Calculated 1 Hz levels range between approximately 95–105 dB at the receptor locations. Depending on atmospheric stability, wind direction, and ground conditions, variations of approximately ± 15 –20 dB may occur.

An infrasound level of 95 dB at 1 Hz corresponds to an integrated broadband level (1–20 Hz) of approximately 103 dB. Several peer-reviewed studies have reported measurable neurophysiological responses at exposure levels between 80–90 dB under controlled laboratory conditions [51, 11]. Given both the calculated exposure levels and the spatial extent of the affected area, these results warrant careful consideration in environmental and public health assessments.

A second simulation was conducted using a representative daytime atmospheric profile with easterly wind conditions of 4 m/s. The corresponding spatial distribution is shown in Figure 5, with receptor levels summarized in Table 3. The comparison clearly demonstrates that atmospheric conditions and wind direction have a significant impact on infrasound propagation, particularly at longer distances from the source.

Uncertainty interpretation: The colored contours represent level intervals including model uncertainty. For example, a contour labeled 95 dB corresponds to approximately $95 \text{ dB} \pm 2.5 \text{ dB}$. This uncertainty primarily reflects variability in ground impedance, atmospheric attenuation, and interference patterns.

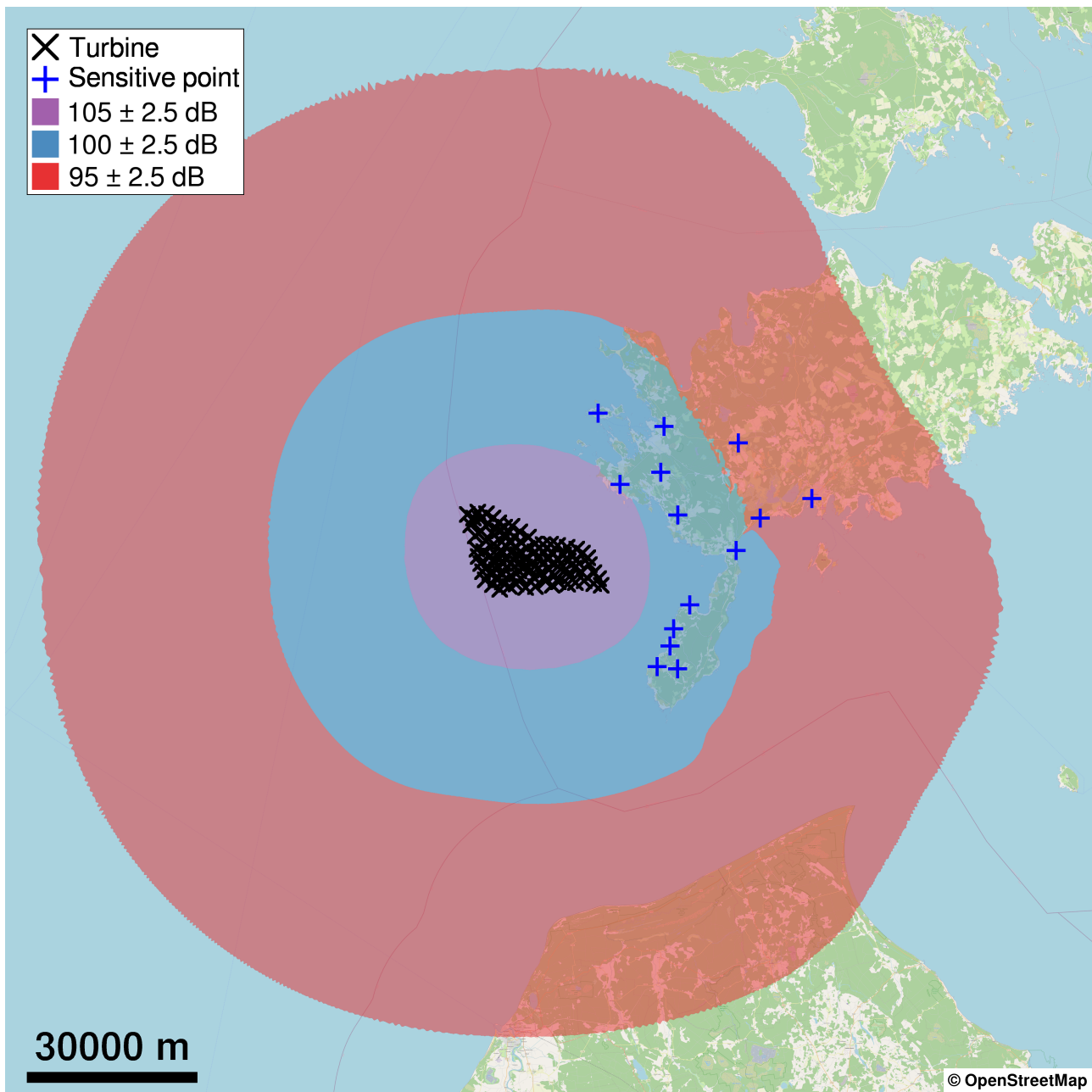


Figure 4: Simulated infrasound levels at 1 Hz (dB) under nighttime atmospheric conditions with a tailwind of 8 m/s. Results are computed using *SoundSim360*. Areas inside the inner red contour correspond to levels ≥ 97.5 dB.

Location	x-coordinate	y-coordinate	SPL (1 Hz) [dB]	Nearest turbine [m]
Vilsandi	373505	6473120	100.4	24127
Kihelkonna	384964	6470470	99.0	26427
Kärla	397891	6467211	96.6	33247
Lümanda	384178	6462440	100.3	19753
Karala	376960	6460525	102.3	13682
Kuressaare	410580	6457144	95.5	40094
Kotlandi	386928	6454850	100.7	17523
Mändjala	401418	6453922	97.0	30382
Salme	397038	6448346	98.3	24567
Rahuste	388585	6438994	100.4	15993
Kaunispe	385619	6434842	100.9	14911
Jämaja	384881	6431822	100.6	16194
Türju	382501	6428239	100.7	17436
Iide	386132	6427762	99.6	19996

Table 2: Calculated infrasound levels at 1 Hz (dB) at representative receptor locations under nighttime conditions (tailwind 8 m/s). Sound power level: 163 dB at 1 Hz.

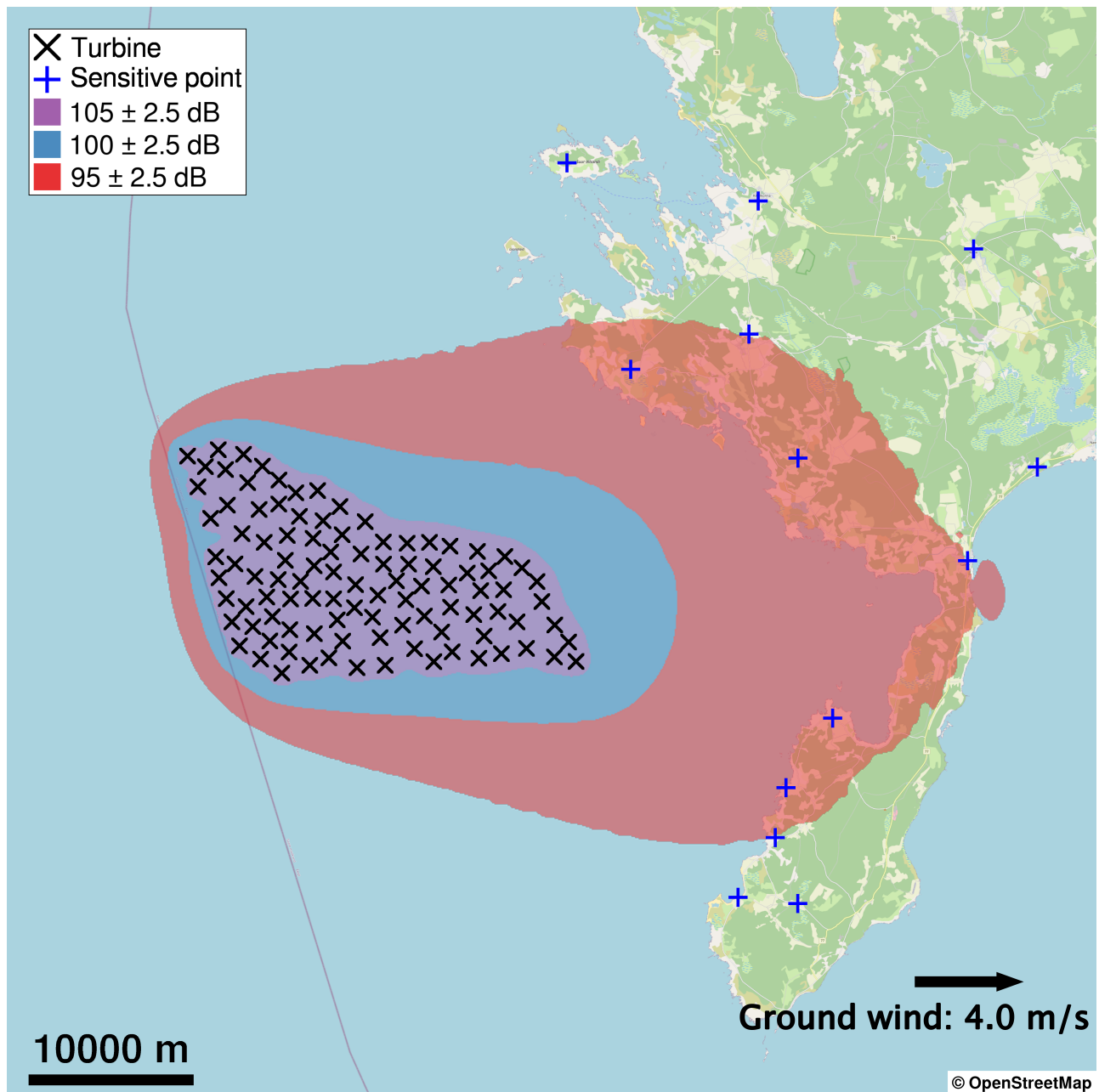


Figure 5: Simulated infrasound levels at 1 Hz (dB) under daytime atmospheric conditions with an easterly wind of 4 m/s. Results are computed using *SoundSim360*. The figure illustrates the sensitivity of infrasound propagation to wind direction and atmospheric structure.

Location	x-coordinate	y-coordinate	SPL (1 Hz) [dB]	Nearest turbine [m]
Vilsandi	373505	6473120	86.4	24127
Kihelkonna	384964	6470470	88.6	26427
Kärla	397891	6467211	89.5	33247
Lümanda	384178	6462440	92.5	19753
Karala	376960	6460525	94.0	13682
Kotlandi	386928	6454850	94.3	17523
Mändjala	401418	6453922	91.5	30382
Salme	397038	6448346	92.5	24567
Rahuste	388585	6438994	93.9	15993
Kaunispe	385619	6434842	93.6	14911
Jämaja	384881	6431822	92.4	16194
Türju	382501	6428239	90.8	17436
Iide	386132	6427762	90.1	19996

Table 3: Calculated infrasound levels at 1 Hz (dB) at representative receptor locations under daytime conditions (easterly wind 4 m/s). Sound power level: 163 dB at 1 Hz.

Conclusions

Our *SoundSim360* simulations for the proposed Saaremaa Offshore Wind Farm indicate that infrasound levels within the inner boundary of the red-marked region in Figure 4 may reach approximately 97.5 dB at 1 Hz. When integrated across the frequency range 1–20 Hz, this corresponds to a broadband infrasound level on the order of 106 dB. The area exposed to levels above 92.5 dB at 1 Hz extends several kilometers from the wind farm.

The corresponding dBA simulations indicate nighttime A-weighted sound pressure levels that are generally consistent with, although in some locations slightly higher than, those presented in the EIA documentation. The predicted levels remain below the discussed 35 dBA nighttime guideline value for sensitive residential environments. However, these results should be interpreted with caution, particularly under stable nighttime atmospheric conditions where amplitude modulation and long-range propagation effects may become more pronounced.

It should be emphasized that predictions of low-frequency and infrasonic sound are subject to uncertainties related to atmospheric conditions, source characterization, terrain effects, and modeling assumptions. In addition, the relationship between narrow-band levels (e.g., at 1 Hz) and broadband metrics should be interpreted with care.

A growing body of peer-reviewed research [8, 39, 40, 41, 51, 11, 16, 35, 42] has investigated physiological, perceptual, and affective responses to infrasonic and low-frequency sound. Some controlled experimental studies report measurable changes in physiological or affective markers under specific exposure conditions, including situations where the sound is not consciously perceived. However, the literature remains heterogeneous, and the magnitude, mechanisms, and long-term implications of such responses remain subjects of ongoing scientific investigation.

Related questions have also been raised in the context of wildlife and animal behavior, where infrasonic acoustic energy has been proposed as a potential contributing factor influencing behavior, stress responses, or navigation. Current evidence in this area remains limited and inconclusive [47, 46].

Wind turbine noise is further characterized by amplitude modulation and temporal variability, including low-frequency components, which may influence perceptual responses differently compared to more stationary environmental noise sources.

Taken together, the modeling results and the existing scientific literature indicate that infrasonic and low-frequency sound may represent relevant components of the acoustic environment that are not fully characterized by standard assessment metrics based primarily on A-weighted sound levels. From a precautionary and scientific perspective, these findings support the need for continued research, improved exposure characterization, independent long-term measurements, and careful consideration of low-frequency and infrasonic components in future environmental impact assessments.

References

- [1] Nina Aguilera, Henrik Naglitsch, and Katrin Olofsson. Beräkningsmanual Nord2000 : för bullerberäkningar i väg-och järnvägsplaner. Technical Report 2024:033, Efterklang, 2024.

- [2] Martin Almquist and Eric M. Dunham. Non-stiff boundary and interface penalties for narrow-stencil finite difference approximations of the laplacian on curvilinear multiblock grids. *Journal of Computational Physics*, 408:109294, 2020.
- [3] Martin Almquist, Ilkka Karasalo, and Ken Mattsson. Atmospheric sound propagation over large-scale irregular terrain. *Journal of Scientific Computing*, 61(2):369–397, 2014.
- [4] Stephen E. Ambrose, Robert W. Rand, and Carmen M. E. Krogh. Wind turbine acoustic investigation: Infrasound and low-frequency noise – a case study. *Bulletin of Science, Technology & Society*, 32(2):128–141, 2012.
- [5] Walker B, Hessler G, Hessler D, Rand R, and Schomer P. *A Cooperative Measurement Survey and Analysis of Low Frequency and Infrasound at the Shirley Wind Farm in Brown County, Wisconsin*. Report number 122412-1, 2012.
- [6] Mathias Basner, Wolfgang Babisch, Adrian Davis, Mark Brink, Charlotte Clark, Sabine Janssen, and Stephen Stansfeld. Auditory and non-auditory effects of noise on health. *The Lancet*, 383(9925):1325–1332, 2014.
- [7] Richard A Carman. Measurement procedure for wind turbine infrasound. In *INTER-NOISE and NOISE-CON Congress and Conference Proceedings*, volume 250, pages 6143–6153. Institute of Noise Control Engineering, 2015.
- [8] Åke Danielsson and Ulf Landström. Blood pressure changes in man during infrasonic exposure. *Acta Medica Scandinavica*, 217(5):531–535, 1985.
- [9] International Organization for Standardization. *Acoustics: Attenuation of Sound During Propagation Outdoors*. International Organization for Standardization, 1993.
- [10] International Organization for Standardization. *Acoustics-Attenuation of Sound During Propagation Outdoors: Part 2: General Method of Calculation*. 1996.
- [11] Caroline Garcia Forlim, Leonie Ascone, Christian Koch, and Simone Kühn. Resting state network changes induced by experimental inaudible infrasound exposure and associations with self-reported noise sensitivity and annoyance. *Scientific Reports*, 14(1):24555, 2024.
- [12] Dan Hoffmeyer and Jørgen Jakobsen. Sound insulation of dwellings at low frequencies. *Journal of Low Frequency Noise, Vibration and Active Control*, 29(1):15–23, 2010.
- [13] N D Kelley, H E McKenna, R R Hemphill, C L Etter, R L Garrelts, and N C Linn. Acoustic noise associated with the mod-1 wind turbine: its source, impact, and control. Technical report, Solar Energy Research Inst. (SERI), Golden, CO (United States), 02 1985.
- [14] Lantmäteriet. Terrain Model Download, grid 1+. <https://www.lantmateriet.se/sv/Kartor-och-geografisk-information/geodataprodukter/produktlista/markhojdmodell-nedladdning-grid-1/>, 2021.
- [15] Conny Larsson. Ljud från vindkraftverk, modell-validering-mätning : Slutrapport Energimyndighetens projekt 32437-1. Technical report, Uppsala University, LUVAl, 2014.
- [16] Francesca Lionetti, Arthur Aron, Elaine N. Aron, G. Leonard Burns, Jadzia Jagiellowicz, and Michael Pluess. Dandelions, tulips and orchids: evidence for the existence of low-sensitive, medium-sensitive and high-sensitive individuals. *Translational Psychiatry*, 8(1):24, 2018.
- [17] L. Liszka. *Infrasound: A Summary of 35 Years of Infrasound Research*. IRF scientific report. Swedish Institute of Space Physics, 2008.
- [18] Lukas Lundgren and Ken Mattsson. An efficient finite difference method for the shallow water equations. *Journal of Computational Physics*, 422:109784, 2020.
- [19] K. Mattsson, M. Almquist, and M. H. Carpenter. Optimal diagonal-norm SBP operators. *Journal of Computational Physics*, 264:91–111, 2014.
- [20] K. Mattsson and M. H. Carpenter. Stable and accurate interpolation operators for high-order multi-block finite-difference methods. *SIAM J. Sci Comput.*, 32(4):2298–2320, 2010.
- [21] K. Mattsson, M. Svärd, M.H. Carpenter, and J. Nordström. High-order accurate computations for unsteady aerodynamics. *Computers & Fluids*, 36:636–649, 2006.

- [22] K. Mattsson, M. Svård, and M. Shoeybi. Stable and accurate schemes for the compressible navier-stokes equations. *Journal of Computational Physics*, 227(4):2293–2316, 2008.
- [23] Ken Mattsson. Summation by parts operators for finite difference approximations of second-derivatives with variable coefficients. *Journal of Scientific Computing*, 51:650–682, 2012.
- [24] Ken Mattsson. Diagonal-norm upwind SBP operators. *Journal of Computational Physics*, 335:283 – 310, 2017.
- [25] Ken Mattsson, Martin Almquist, and Edwin van der Weide. Boundary optimized diagonal-norm SBP operators. *Journal of Computational Physics*, 2018.
- [26] Ken Mattsson, Gustav Eriksson, Leif Persson, José Chilo, and Kourosh Tatar. Efficient finite difference modeling of infrasound propagation in realistic 3D domains: Validation with wind turbine measurements. *Applied Acoustics*, 243:111156, 2026.
- [27] Ken Mattsson, Frank Ham, and Gianluca Iaccarino. Stable and accurate wave-propagation in discontinuous media. *Journal of Computational Physics*, 227(19):8753–8767, 2008.
- [28] Ken Mattsson, Frank Ham, and Gianluca Iaccarino. Stable boundary treatment for the wave equation on second-order form. *Journal of Scientific Computing*, 41(3):366–383, 2009.
- [29] Ken Mattsson and Ylva Ljungberg Rydin. Implicit summation by parts operators for finite difference approximations of first and second derivatives. *Journal of Computational Physics*, 473:111743, 2023.
- [30] Ken Mattsson and Jan Nordström. High order finite difference methods for wave propagation in discontinuous media. *Journal of Computational Physics*, 220(1):249–269, 2006.
- [31] Ken Mattsson and Pelle Olsson. An improved projection method. *Journal of Computational Physics*, 372:349 – 372, 2018.
- [32] Henrik Möller and Christian Sejer Pedersen. Low-frequency noise from large wind turbines. *The Journal of the Acoustical Society of America*, 129(6):3727–3744, 2011.
- [33] Henrik Møller, Steffen Pedersen, Kerstin Persson Waye, and Christian Sejer Pedersen. Comments to the article "sound insulation of dwellings at low frequencies" i. *Journal of Low Frequency Noise, Vibration and Active Control*, 30(3):229–231, 2011.
- [34] Pelle Olsson, Gustav Eriksson, and Ken Mattsson. Projection based summation-by-parts methods, embeddings and the pseudoinverse. *Journal of Computational Physics*, 524:113689, 2025.
- [35] M. Pluess, E. Assary, F. Lionetti, K. J. Lester, E. Krapohl, E. N. Aron, and A. Aron. Environmental sensitivity in children: Development of the highly sensitive child scale and identification of sensitivity groups. *Translational Psychiatry*, 54(1):51–70, 2018.
- [36] Ylva Rydin, Ken Mattsson, and Jonatan Werpers. High-fidelity sound propagation in a varying 3D atmosphere. *Journal of Scientific Computing*, 77(2):1278–1302, 2018.
- [37] Saare Wind Energy OÜ. Environmental impact assessment program for the saaremaa offshore wind farm. <https://swe.ee/EIA/SWE%20WF%20EIA%20program%2030.03.2021%20ENG.pdf>, March 2021. Environmental Impact Assessment (EIA) Program, 30 March 2021.
- [38] Saare Wind Energy OÜ. Summary of the environmental impact assessment report for the saaremaa offshore wind farm. https://swe.ee/EIA/SWE_EIA_report_Summary_14.08.2023_ENG.pdf, August 2023. Environmental Impact Assessment (EIA) Report Summary, 14 August 2023.
- [39] Alec N. Salt and Timothy E. Hullar. Responses of the ear to low frequency sounds, infrasound and wind turbines. *Hearing Research*, 268(1):12–21, 2010.
- [40] Alec N. Salt and James A. Kaltenbach. Infrasound from wind turbines could affect humans. *Bulletin of Science, Technology & Society*, 31(4):296–302, 2011.
- [41] Alec N Salt and Jeffery T Lichtenhan. How does wind turbine noise affect people. *Acoustics Today*, 10(1):20–28, 2014.
- [42] Kale R. Scatterty, Dawson VonStein, Lisa B. Prichard, Brian C. Franczak, Trevor J. Hamilton, and Rodney M. Schmaltz. Infrasound exposure is linked to aversive responding, negative appraisal, and elevated salivary cortisol in humans. *Frontiers in Behavioral Neuroscience*, Volume 20 - 2026, 2026.

- [43] Bo Søndergaard. Low frequency noise from wind turbines: Do the danish regulations have any impact? an analysis of noise measurements. *International Journal of Aeroacoustics*, 14(5-6):909–915, 2015.
- [44] Vidar Stiernström, Martin Almquist, and Ken Mattsson. Boundary-optimized summation-by-parts operators for finite difference approximations of second derivatives with variable coefficients. *Journal of Computational Physics*, 491:112376, 2023.
- [45] Vidar Stiernström, Lukas Lundgren, Murtazo Nazarov, and Ken Mattsson. A residual-based artificial viscosity finite difference method for scalar conservation laws. *Journal of Computational Physics*, 430:110100, 2021.
- [46] Michael Stocker. Infrasonic acoustic energy produced by offshore wind turbine energy generation may interfere with bird and cetacean navigation cues. *Environmental Science and Pollution Research*, 2026.
- [47] Anne Tolvanen, Henri Routavaara, Mika Jokikokko, and Parvez Rana. How far are birds, bats, and terrestrial mammals displaced from onshore wind power development? – a systematic review. *Biological Conservation*, 288:110382, 2023.
- [48] Antoine Turquet, Quentin Brissaud, Celso Alvizuri, Sven Peter Näsholm, Alexis Le Pichon, and Johan Kero. Retrieving seismic source characteristics using seismic and infrasound data: The 2020 ML 4.1 kiruna minequake, sweden. *Geophysical Research Letters*, 51(12), 2024.
- [49] Wenjie Wang, Yan Yan, Yongnian Zhao, and Yu Xue. Studies on the experimental measurement of the low-frequency aerodynamic noise of large wind turbines. *Energies*, 17(7), 2024.
- [50] Kerstin Persson Waye, Michael Smith, and Mikael Ögren. Hälsopåverkan av lågfrekvent buller inomhus. Technical Report 3, Sahlgrenska Akademin Medicinska Institutionen, 2017.
- [51] Markus Weichenberger, Martin Bauer, Robert Kühler, Johannes Hensel, Caroline Garcia Forlim, Albrecht Ihlenfeld, Bernd Ittermann, Jürgen Gallinat, Christian Koch, and Simone Kühn. Altered cortical and subcortical connectivity due to infrasound administered near the hearing threshold - evidence from fmri. *PLOS ONE*, 12(4):1–19, 04 2017.